Oxidative Charge Transfer To Repair Thymine Dimers and Damage Guanine Bases in DNA Assemblies Containing Tethered Metallointercalators†

Peter J. Dandliker,‡ Megan E. Núñez, and Jacqueline K. Barton*

Division of Chemistry and Chemical Engineering, California Institute of Technology, Pasadena, California 91125

Received January 7, 1998; Revised Manuscript Received March 5, 1998

ABSTRACT: Potent oxidants which intercalate in DNA serve as tools to probe DNA-mediated electron-transfer reactions. A photoexcited rhodium intercalator, $Rh(phi)_2DMB^{3+}$ (phi = 9,10-phenanthrenequinone diimine and DMB = 4,4′-dimethyl-2,2′-bipyridine), tethered to DNA, promotes both oxidative damage to 5′-GG-3′ doublets in DNA and the repair of thymine dimers from a remote site on the DNA duplex. DNA-mediated repair of a thymine dimer lesion by charge transfer from the tethered rhodium intercalator is quantitative, albeit with low photoefficiency, occurs in an intraduplex reaction over long range (36 Å), and requires that the intervening bases be paired. When both oxidative reactions, repair and oxidative damage, are monitored on the same duplex, competition is evident; the presence of both a 5′-GG-3′ site and the thymine dimer diminished the dimer repair efficiency by 20−40% and decreased damage at the 5′-GG-3′ sites 2-fold compared to similar sequences lacking either the guanine doublet or thymine dimer, respectively. In addition to damage at the 5′-G of 5′-GG-3′ sites, we also observe oxidation at the 3′-G of the 5′-GT<>TG-3′ tetrad only in the presence of thymine dimer. Overall, the yield of repaired thymine strand was at least 10 times higher than the yield of oxidized guanine in the same sequences. While the 5-GG-3′ may represent the thermodynamically favored site for oxidative reaction, repair of the thymine dimer appears to be kinetically more favorable. Dipyridophenanzine (dppz) complexes of ruthenium-(III), less potent oxidants which intercalate in DNA, oxidize 5′-GG-3′ doublets efficiently but cannot trigger the repair of the thymine dimer lesion. Oxidative damage to DNA from a distance, mediated by the DNA base pair stack, can, however, be utilized to probe the disruption in the base stack generated by the thymine dimer. The presence of the dimer does not diminish oxidation by a Ru(III) intercalator at a distal guanine doublet, suggesting that the disruption caused by the dimer does not block charge transfer through the DNA duplex. DNA-mediated electron-transfer reactions of metallointercalators therefore serve to illustrate important aspects of radical migration and its consequence with respect to reactions at a distance through the DNA base pair stack.

The DNA double helix is a stacked array of aromatic heterocyclic base pairs. The possibility that the base pairs within this molecular π-stack are electronically coupled and able to facilitate long-range charge transfer is now subject to both theoretical and experimental scrutiny. Early models predicted that charges could hop from base to base, imparting conductivity to the DNA chain (*1*). Using high-energy radiation to ionize DNA, radiation biologists have studied the formation of nucleobase radicals (*2*−*9*) and charge trapping by intercalated radical traps (*10*−*13*). Despite an extensive body of work, estimates of the distance over which radicals migrate through the stacked DNA base pairs range from as few as 2 to as many as 200 base pairs (bp) (*14*). Photoinduced electron transfer through the DNA double helix between bound donor and acceptor molecules has been observed spectroscopically. In these photophysical studies, the DNA acts as a bridge for the charge transfer but does not undergo a chemical reaction (*15*−*28*). Results in our laboratory indicate that efficient DNA-mediated charge transfer is facilitated by intercalation of the reactants and is exquisitely sensitive to π-stacking of both the bases and the intercalated metal complex.

Radical reactions with the DNA bases can also yield irreversible DNA lesions. The importance of oxidative charge transfer in the context of DNA damage has prompted the development of model systems in which small molecules, such as substituted anthraquinones (*29*−*32*), naphthalimide derivatives (*33*), ethidium bromide with methyl viologen (*34*), and riboflavin (*35*), were used to oxidize DNA photochemically. In all of these systems, damage occurred principally at guanine (G), the most easily oxidized base, suggesting that redox potential is an important factor in determining the products which eventually result from the charge trapping event.

We have employed metallointercalators tethered to one end of DNA assemblies to carry out chemical reactions at distant sites on the assemblies. Photoexcited rhodium intercalators such as $Rh(phi)_2DMB^{3+}$ (phi = 9,10-phenanthrenequinone diimine and DMB = 4,4′-dimethyl-2,2′-bipyridine) oxidatively damage DNA selectively at the 5′-G

† This work was supported by a grant from the NIH (GM49216), as well as by a postdoctoral fellowship to P.J.D. from the Damon Runyon Walter Winchell Cancer Fund and a predoctoral fellowship to M.E.N. from the Howard Hughes Medical Institute.

* To whom correspondence should be addressed.

‡ Current address: Abbott Laboratories, Abbott Park, IL, 60064.

S0006-2960(98)00041-5 CCC: $15.00
Published on Web 04/08/1998

of 5′-GG-3′ sites to form 8-oxo-2′-deoxyguanosine (8-oxo-dG), the primary oxidative lesion to DNA within the cell (*36*−*38*).[1] We showed that rhodium intercalators tethered to one end of a DNA duplex induced oxidative damage specifically at the 5′-G of 5′-GG-3′ sites located at least 34 Å away in the duplex (*38*). The selectivity for 5′-GG-3′ doublets agrees with ab initio calculations which indicate that the HOMO is localized on the 5′-G (*39*). Furthermore, when a DNA assembly was constructed containing the tethered rhodium intercalator, and two 5′-GG-3′ charge trapping sites were separated by an intervening DNA bulge, oxidative reaction at the distal site was diminished relative to the proximal 5′-GG-3′ doublet (*37*). These data illustrated the sensitivity of DNA-mediated charge transfer to the integrity of the intervening base pair stack.

Oxidative damage to DNA from a distance is observed in high yield in DNA assemblies containing tethered ruthenium oxidants (*40*, *41*). In these studies, a ground-state ruthenium(III) oxidant is generated in situ by photoinduced quenching of ruthenium(II) by a groove-bound quencher such as methyl viologen or $Ru(NH_3)_6^{3+}$. Transient absorption spectroscopy with $Ru(phen)_2dppz^{3+}$ allowed the identification of the neutral guanine radical intermediate in poly dGC (*41*). Moreover, in DNA assemblies with the tethered oxidant, mismatch studies served to underscore the presence of charge migration across the base pair stack on a time scale which is fast compared to the trapping time for irreversible oxidation of the guanine radical to form the product 8-oxo-dG (*40*).

The thymine cyclobutane dimer (T<>T) is a DNA lesion which results from a [2+2] photocycloaddition between adjacent thymine bases on the same polynucleotide strand (*42*). Bacteria use photolyase enzymes with bound flavin cofactors to repair the thymine lesion in a reductive catalytic cycle upon visible irradiation (*43*−*47*). The repair of thymine dimers triggered both oxidatively and reductively has been shown in model systems (*48*−*52*). Most recently, Carrell and co-workers demonstrated cleavage of pyrimidine photodimers by covalently attached reduced flavins (*53*, *54*). We demonstrated that photoexcited rhodium oxidants tethered to DNA can promote the repair of thymine dimer lesions located at least 26−36 Å away in the DNA base stack via a long-range oxidative electron-transfer process (*55*).

Here, we describe thymine dimer repair by photoexcited metallointercalators in more detail. Additionally, we explore the relative reactivity of the thymine dimer and guanine doublet in a single duplex and allow sites to compete for trapping of the mobile charge. The guanine doublet and the thymine dimer are expected to localize a mobile charge to different extents: the oxidation potential of guanine is approximately +1.3 V at neutral pH (*56*), while the standard oxidation potential of the thymine dimer is around +2.0 V (*57*−*59*). Furthermore, the trapped radical intermediates formed at the two sites have distinctly different intrinsic lifetimes and stabilities. Hence, in an assembly containing both sites, it becomes interesting to explore their relative reactivities. Metallointercalators offer useful tools to probe this DNA-mediated charge-transfer chemistry and more generally to begin to characterize radical migration through a DNA base pair stack.

[1] Abbreviations: T<>T, thymine dimer; 8-oxo-dG, 8-oxo-2′-deoxyguanosine; phi, 9,10-phenanthrenequinone diimine; DMB, 4, 4′-dimethyl-2,2′-bipyridine; phen, 1,10-phenanthroline; dppz, dipyrido[3,2-a:2′,3′-c]phenazine; bpy′, 4-butyric acid-4′-methylbipyridine.

EXPERIMENTAL PROCEDURES

Materials. Oligonucleotides were prepared on an Applied Biosystems 394 DNA synthesizer, using phosphoramidite chemistry (*60*−*62*). DNA was synthesized with a 5′-dimethoxy trityl protective group and was purified by HPLC on a Dynamax 300 Å C_{18} reversed-phase column (10 mm i.d. × 25 cm length) from Rainin on a Hewlett-Packard 1090 HPLC. The DNA was deprotected by incubation with 80% CH_3COOH for 20 min at 20 °C and HPLC purified again. Duplexes were formed by cooling (linear gradient) solutions containing equimolar quantities of complementary oligonucleotides from 95 to 20 °C over 90 min. $Rh(phi)_2DMB^{3+}$, $Ru(phen)_2dppz^{2+}$ (dppz = dipyrido[3,2-a:2′,3′−c]phenazine), $Rh(phi)_2(bpy')^{3+}$ (bpy′ = 4-butyric acid-4′-methylbipyridine), and $Ru(phen)(bpy')(dppz)^{2+}$ were prepared according to published procedures (*63*−*65*). Rhodium-modified oligonucleotides were prepared according to published procedures (*38*, *55*). Characterization included mass spectrometry, base digestion, UV/visible spectrophotometry, and melting temperature determination, as previously described. The electron-transfer quenchers methyl viologen dichloride, $[Ru(NH_3)_6]Cl_3$, and $[Co(NH_3)_5Cl]Cl_2$ were purchased from Aldrich Chemical Co. and used as received. Acetophenone was recrystallized three times before use and stored at 4 °C in the dark. The concentration of single-stranded oligonucleotides in aqueous solution was determined by UV−visible spectroscopy on a Beckman DU 7400 Spectrophotometer; ϵ(260 nm, M^{-1} cm^{-1}) adenine (A) = 15 400; guanine (G) = 11 500; cytosine (C) = 7 400; thymine (T) = 8 700; thymines in thymine dimer (TT) = 0; for Rh-modified oligonucleotides, ϵ(390 nm M^{-1} cm^{-1}) = 19 000; for Ru-modified oligonucleotides, ϵ(442 nm M^{-1} cm^{-1}) = 19 000. For metal complexes: $Rh(phi)_2DMB^{3+}$, ϵ(350 nm M^{-1} cm^{-1}) = 23 600, pH isosbestic; $Ru(phen)_2dppz^{2+}$, ϵ(440 nm M^{-1} cm^{-1}) = 21 000.

Preparation and Characterization of Oligonucleotides Containing a Thymine Dimer. Thymine dimer formation in synthetic oligonucleotides was performed photochemically, using acetophenone as a triplet photosensitizer (*66*, *67*). Sequences contained only a single TT site and no other adjacent pyrimidine bases. Aqueous solutions (1 mL) containing the oligonucleotide (~0.2 mM) and acetophenone (25 mM) were placed in an evacuable irradiation apparatus and rigorously degassed by freezing the sample, applying a vacuum, and slow thawing. This process was repeated six times for each sample. Solutions were irradiated in vacuo for 4−6 h (λ = 330 nm) with a 1000 W Hanovia Hg−Xe arc lamp equipped with a monochromator. Products were purified by HPLC on a Dynamax 300 Å C_{18} reversed-phase column (10 mm i.d. × 25 cm L) from Rainin using a Hewlett-Packard 1090 HPLC. The strands eluted with a gradient of 50 mM CH_3COONH_4 (pH 6.5)/CH_3CN (~93:7 to ~89:11 over 30 min, flow rate = 3.5 mL min^{-1}). In all cases, the desired thymine dimer-containing compound eluted ~2 min before the unreacted starting material, and was formed as the major product. The product ratios are consistent with those previously reported and support the assignment of the major product as the cis-syn isomer (*66*).

Conversion for 16-nucleotide strands ranged from 30 to 50%. Purity of the material was confirmed by analytical HPLC.

The presence and identity of the thymine dimer were confirmed using electrospray ionization-Fourier transform ion cyclotron resonance mass spectroscopy (ESI-FTICR MS), enymatic digestion, and direct photoreversal to the normal oligonucleotide without the dimer. As expected, an oligonucleotide containing a repaired thymine dimer had a mass identical to that of the parent material as determined by electrospray ionization mass spectrometry. The theoretical mass of a 16-base-pair oligonucleotide with a repaired thymine dimer was 4929.8 (*55*), while the experimental mass of the repaired dimer strand was 4929.4. The identity of a thymine cyclobutane dimer can also be confirmed by direct photoreversal. Treatment of thymine dimer-containing DNA with 254 nm light, which is known to repair this type of lesion, afforded a compound with the same retention time as the original oligonucleotide (*68*). T4 DNA polymerase possesses 3′−5′ exonuclease activity which is blocked by the presence of a thymine dimer. Digestion of 5′-^{32}P-labeled thymine dimer strands with T4 DNA polymerase gave only products in which enzymatic cleavage was arrested at the site of thymine dimer incorporation. As expected, thymine dimer-containing DNA was not susceptible to cleavage with hot piperidine, a treatment which is known to cleave DNA containing the pyrimidine-pyrimidone (6-4) photoproduct (*69*).

HPLC Assay for Thymine Dimer Repair. Complementary DNA strands were hybridized in aerated buffer containing 50 mM sodium chloride and 5 mM sodium phosphate, pH 8.0. Oligonucleotide duplexes (8 μM) containing tethered Rh(phi)$_2$bpy′$^{3+}$ were irradiated at 365 nm for 1 and 3 h. Lamp power, monitored at $\lambda = 325$ nm on a model 45 laser power meter (LiCONiX), was ∼40 mW. For experiments with Ru(phen)$_2$dppz^{2+}, oligonucleotide duplexes (8 μM) containing Ru(phen)$_2$dppz^{2+} (8 μM) and 10 equiv of methyl viologen were irradiated at 436 nm for 2 and 5 min Lamp power, monitored at $\lambda = 442$ nm, was ∼8.9 mW. Reaction mixtures were analyzed by HPLC on a Microsorb-MV C_{18} reversed-phase column (4.6 mm i.d. × 25 cm length) from Rainin maintained at 65 °C, eluting with a gradient of 20 mM CH_3COONH_4, (pH 6.5)/CH_3CN (98:2 to 93:7 over 20 min, isocratic at 93:7 for 5 min, to 50:50 over 5 min, isocratic at 50:50 for 5 min; flow rate = 1.0 mL min^{-1}). Under these conditions, the duplexes dissociate into single stranded components, each of which elutes from the column with a distinct retention time. Oligonucleotides (16 nucleotide) containing a thymine dimer eluted first (∼11−12 min), followed by the corresponding repaired strand (∼15−16 min), and the complement with tethered rhodium (∼30 min). Identity of the individual compounds was confirmed by coinjection with authentic material and, in one case, by isolation and electrospray ionization mass spectrometric analysis of the repaired strand. Thymine dimer repair was quantitated from peak areas in the chromatograms (normalized for differences in molar absorptivity at the detection wavelength, $\lambda = 260$ nm).

Preparation of Ruthenium-Modified Oligonucleotides. Ruthenium-modified oligonucleotides were prepared as follows. To a stirring solution of racemic [Ru(phen)(bpy′)(dppz)]Cl_2 (6 mg, 6.7 μmol) in $CH_3CN/CH_2Cl_2/CH_3OH$ (1:1:1) at 20 °C was added *O*-(*N*-succinimidyl)-*N*,*N*,*N*′,*N*′-tetramethyluronium tetrafluoroborate (8 mg, 26 μmol) and *N*-ethyldiisopropylamine (3 μL, 18 μmol). After 1 h, the orange-red solution and *N*-ethyldiisopropylamine (10 μL, 58 μmol) were stirred with 2000 Å controlled pore glass (CPG) bearing the protected oligonucleotide, which had been previously functionalized at its free 5′-OH with a −CONH-$(CH_2)_9NH_2$ linker (2 μmol DNA synthesis). The linker-functionalized DNA was prepared as previously described (*70*). After 12 h, the orange CPG was washed with CH_3CN (5 × 3 mL), CH_3OH (10 × 3 mL), and CH_2Cl_2 (5 × 3 mL), dried under vacuum, and incubated with concentrated NH_4-OH (0.75 mL) at 55 °C for 6 h to affect deprotection and cleavage of the conjugate from the solid support. The [Ru(phen)(bpy′)(dppz)]Cl_2 sample used in the coupling consisted of two positional isomers, each existing as either the Δ or Λ stereoisomer; four conjugation products were therefore observed. The four desired Ru−oligonucleotide conjugates were purified by HPLC on a Dynamax 300 Å C_{18} reversed-phase column (10 mm i.d. × 25 cm length) from Rainin using a Hewlett-Packard 1090 HPLC. The strands eluted with a gradient of 20 mM CH_3COONH_4 (pH 6.5)/CH_3CN (∼93:7 to ∼89:11 over 30 min, to 50:50 over 5 min, flow rate = 3.5 mL min^{-1}). Absolute configuration about the metal center was determined by circular dichroism spectroscopy based on the stereochemistry of the metal center (*71*). Racemic metal complexes were used for all experiments involving metallointercalators bound noncovalently to DNA; single diastereomers of the metal−oligonucleotide conjugates, named 1Δ and 4Δ to indicate the configuration and order of elution, were used in experiments with tethered complexes.

PAGE Assay for Oxidative Damage. Oligonucleotides were enzymatically phosphorylated (*) at the 5′-OH with [γ-^{32}P]ATP according to a standard protocol (*72*). The product was purified by C_{18} chromatography on a Nensorb 20 cartridge (NEN Research Products), freed of solvent in vacuo, incubated at 90 °C with 10% aqueous piperidine (0.100 mL) for 30 min, dried, and electrophoresed on a denaturing 20% polyacrylamide gel (0.8 mm thickness). Labeled product was located in the gel by autoradiography, excised, and extracted by incubation at 37 °C with 90 mM Tris-borate buffer (pH 8.3) containing 1 mM EDTA for 12 h. The mixture was filtered through an uncharged nylon-66 membrane, 0.45 μM pore size (Rainin), desalted on a Nensorb 20 cartridge, and freed of solvent in vacuo. Complementary DNA strands were hybridized in aerated buffer containing 5 mM sodium phosphate and 50 mM sodium chloride, pH 8.5. Oligonucleotide duplexes (8 μM) containing tethered Rh(phi)$_2$bpy′$^{3+}$ were irradiated at 365 nm for 1 and 3 h (lamp power, monitored at $\lambda = 325$ nm, ∼40 mW), incubated at 90 °C with 10% aqueous piperidine (0.100 mL) for 30 min, dried, and electrophoresed on a denaturing 20% polyacrylamide gel (0.4 mm thickness). Cleavage of the labeled strand was quantitated by phosphorimagery using ImageQuant, v.3.3 software (Molecular Dynamics). Oxidation at individual bases was determined by measuring the intensity of the band corresponding to that base as a fraction of the intensity of the whole lane. The fractional intensity of the corresponding band in the control lane was subtracted out to account for background damage.

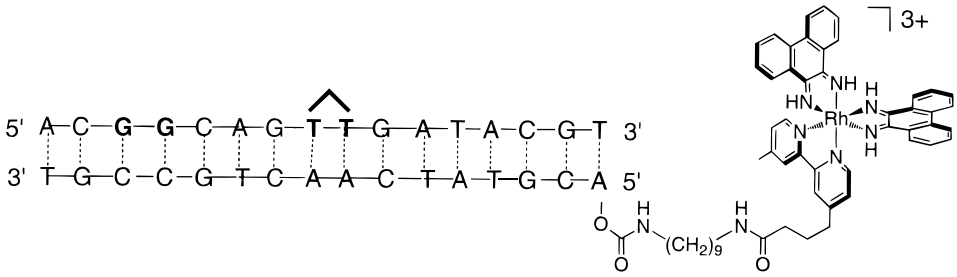

FIGURE 1: Example of a DNA assembly tethered to $Rh(phi)_2(bpy')^{3+}$, showing the structure of the linker and the metal ligands. The sequence at the intercalation site, the total AT/GC content, and the sequence around the surrounding the two oxidizable sites are the same in all of the assemblies.

RESULTS

Sequence Construction. We designed and constructed a family of DNA duplexes containing a tethered rhodium intercalator, a 5′-GG-3′ site, and a thymine dimer lesion. Figure 1 illustrates their general formulation. The sequences vary with respect to the presence or absence of a 5′-GG-3′ site and a thymine dimer lesion, as well as their relative position with respect to the tethered oxidant. The assemblies possess an equivalent base composition (G/C and A/T content). The conserved 5′-···ATACGT-3′ sequence at the tethered end provides a uniform DNA binding site for the metal complexes throughout the series. Bases immediately flanking the 5′-GG-3′ and thymine dimer sites are also conserved in an effort to maintain structural uniformity at these sites from duplex to duplex.

DNA oligonucleotides with appended $Rh(phi)_2bpy'^{3+}$ were prepared by solid phase synthesis, and oligonucleotides with thymine dimer lesions were prepared by photolysis of single stranded DNA as previously described (*38*, *55*). The strands were purified and characterized by UV−visible spectroscopy, circular dichroism, base digestion, or mass spectrometry before the complete duplex assemblies were formed by annealing the thymine-dimer containing strands to metalated (or nonmetalated) strands.

Determination of Metal-Binding Sites via Photocleavage. Photocleavage reactions permit us to determine the positions at which the metal complexes bind to the DNA duplex. High-energy (313 nm) photoexcitation of phi complexes of rhodium bound to DNA promotes direct strand cleavage in a reaction consistent with C3′ hydrogen atom abstraction at ribose and subsequent strand scission at the intercalation site(s); the base is not oxidized in the photocleavage reaction, as revealed by HPLC, MS, and chemical degradation of the products. (*73*−*75*).

Metalated DNA duplexes containing a 5′-^{32}P-endlabel on the unmetalated strand were irradiated at 313 nm and electrophoresed on a denaturing polyacrylamide gel (Figure 2). In this experiment, all samples were treated with piperidine prior to electrophoresis. Here high-energy irradiation yields strand cleavage by direct reaction at the sugar, while irradiation at lower energy (365 nm) shows the products of both direct photocleavage and base oxidation (vide infra). Lanes 4, 8, 12, and 16 show the photocleavage reactions at 313 nm. The primary cleavage, evident at the top of the gel, occurs at the first four bases, indicating that the rhodium is intercalated at the end furthest from the label. Since the photocleavage reaction at high energy (313 nm), involving direct reaction at the sugar, generates no diffusible species, the multiple cleavage sites observed reflect multiple binding sites for the tethered rhodium. Thus, intercalation is indicated up to four base steps from the end of the duplex, consistent with the flexibility and length of the tether.[2]

It is noteworthy that, for the duplexes containing the thymine dimer, direct contact between the metal complex and the dimer is not required for repair. If $Rh(phi)_2(DMB)^{3+}$ bound noncovalently to DNA is irradiated at 313 nm, photocleavage is seen throughout the duplex (data not shown). Furthermore, on the basis of the photocleavage results, tethering of rhodium to the end of the duplex precludes direct contact of the metal center with the thymine dimer.

For the sequences in Figure 2, we calculate the distance from the intercalated rhodium to the thymine dimer to be approximately 19 Å (**T**<>**T-1**, **T**<>**T-2**) and 36 Å (**T**<>**T-3**, **T**<>**T-4**), measured through the DNA base stack from the third base step (the most probable intercalation site) to the center of the cyclobutane ring of the dimer. This assumes that the centroid-to-centroid stacking distance between adjacent base pairs is 3.4 Å.

Long-Range Oxidative Guanine Damage in the Presence of a Thymine Dimer. Oxidative damage at the 5′-G of 5′-GG-3′ sites in **1**, **T**<>**T-1**, **3**, and **T**<>**T-3** was monitored as a function of irradiation at 365 nm and the results are also illustrated in Figure 2. As expected, oxidative damage, indicated by arrows, is observed at the 5′-G of guanine doublets in sequences both with a dimer and without a dimer. Given that the rhodium intercalates next to the third base pair, oxidative damage is seen at a distance of 37 and 20 Å, respectively, from the tethered oxidant. In addition to damage at the 5′-G of 5′-GG-3′ sites, we also observe oxidation at the 3′-G of the 5′-GT<>TG-3′ tetrad only in the presence of dimer (lanes 5−7 and 13−15).

The amounts of damage at the 5′-G of the guanine doublets, quantitated by phosphorimagery, are given in Table 1. The amount of guanine damage is twice as large when the 5′-GG-3′ site is located distally from the intercalated rhodium (37 Å) than it is when the 5′-GG-3′ site is located proximally (20 Å). This is apparent both in the absence (**1** and **3**) and the presence (**T**<>**T-1** and **T**<>**T-3**) of the thymine dimer. However, the presence of the thymine dimer produced a 2-fold diminution in oxidative damage in the corresponding assemblies, **T**<>**T-1** and **T**<>**T-3** relative to **1** and **3**, respectively.

Analysis of these data, however, is complicated by rhodium-induced thymine dimer repair which precedes or

[2] Upon the basis of modeling, a more restrictive tether would not permit full intercalation.

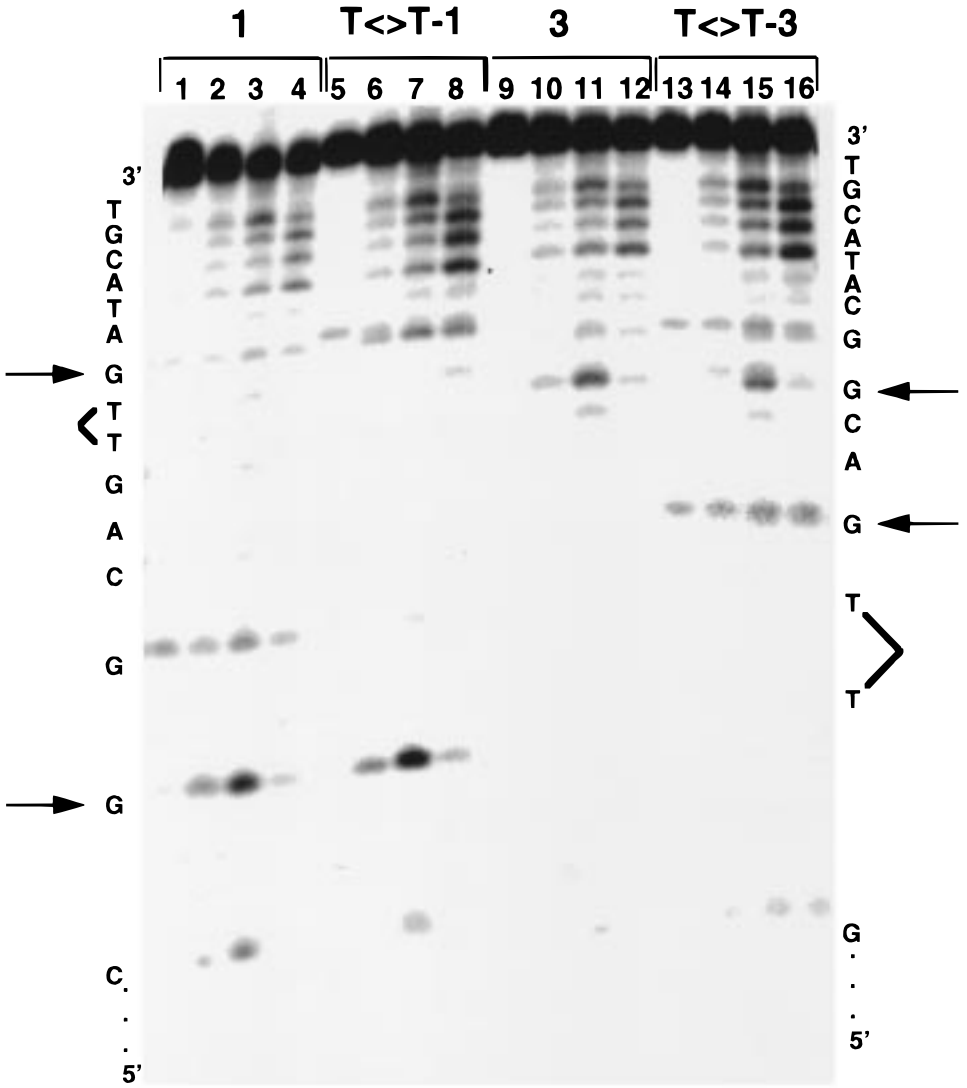

FIGURE 2: Autoradiogram of 5′-[^{32}P]-ACGGCAGTTGATACGT-3′ (duplex **1**), 5′-[^{32}P]-ACGGCAGT<>TGATACGT-3′ (duplex **T<>T-1**), 5′-[^{32}P]-AGTTGACGGCATACGT-3′ (duplex **3**), and 5′-[^{32}P]-AGT<>TGACGGCATACGT-3′ (duplex **T<>T-3**), after photoinduced oxidation of the oligonucleotide duplex by tethered $Rh(phi)_2bpy'^{3+}$ and treatment with aqueous piperidine. Lanes contain the following samples: lanes 1−4, sequence **1** after 0, 1, and 3 h irradiation at 365 nm or 20 min at 313 nm, respectively; lanes 5−8, sequence **T<>T-1** after 0, 1, and 3 h irradiation at 365 nm or 20 min at 313 nm, respectively; lanes 9−12, sequence **3** after 0, 1, and 3 h irradiation at 365 nm or 20 min at 313 nm; lanes 13−16, sequence **T<>T-3** after 0, 1, and 3 h irradiation at 365 nm or 20 min at 313 nm. Horizontal arrows denote the 5′-G of 5′-GG-3′ and the 3′-G of 5′-GTTG-3′ sites. Position of the thymine dimer lesion is denoted by brackets.

is concurrent with the oxidative damage. Over the first hour of this irradiation, we estimate that 50−70% of the thymine dimer lesions are repaired (vide infra). That damage occurs at the 3′-side of the thymine dimer confirms that the dimer is present at least part of the time during the course of reaction.

*Repair of Thymine Dimers in Duplex DNA by *Rh(III).* In assemblies containing both a tethered rhodium intercalator and a thymine dimer lesion, low energy (365 nm) excitation promotes the repair of the lesion triggered through long-range oxidative electron transfer. Thymine dimer repair was measured as a function of irradiation time by reversed-phase analytical HPLC at 65 °C (Figure 3A). Under these conditions, the duplexes melt and each single-stranded oligonucleotide component elutes with a characteristic retention time. The rhodium-tethered strand is not evident in the HPLC trace shown in Figure 3A because it elutes much later in the gradient. No other products besides the dimer-containing strand and the repaired strand are formed in the repair reaction, as monitored by HPLC. We obtain quantitative conversion of the thymine cyclobutane dimer to the repaired strand containing two unmodified thymines in all cases. Repair requires the presence of both rhodium and light.

Tethered rhodium intercalators repair thymine dimers with a quantum yield of 2×10^{-6} mol/einstein at 400 nm (*55*), while intercalators bound noncovalently repair the dimers more efficiently, with a quantum yield of 1×10^{-4} mol/einstein. These low values are consistent with the poor overall efficiency of rhodium photochemistry. Photoaquation of $Rh(phi)_2DMB^{3+}$, for example, occurs with a photoefficiency of 5×10^{-6} mol/einstein at 365 nm (*38*). Given also that quantitative DNA repair is obtained, the poor photoefficiency appears, then, to reflect the low excited state population of the rhodium complex rather than a small population of DNA assemblies being available for repair.

Thymine dimer repair yields were measured as a function of duplex concentration over a range of concentrations from 25 to 3 μM. Over this concentration range, the yield of repaired strand varied by approximately 17%. Figure 3B

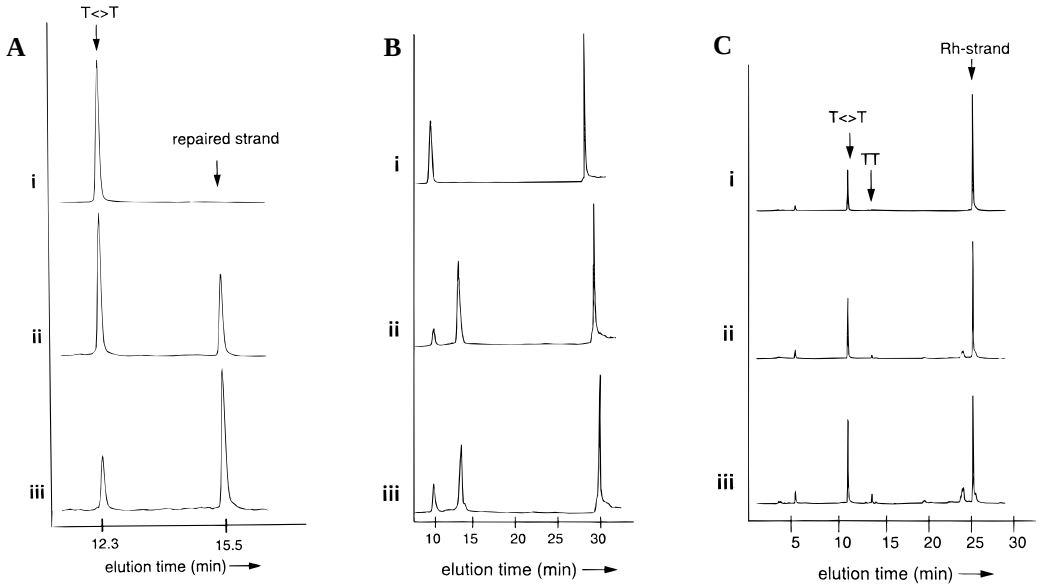

FIGURE 3: (A) Long-range thymine dimer repair in a DNA assembly containing a tethered rhodium intercalator **(T<>T-3)**. Shown are representative HPLC chromatograms at (i) 0, (ii) 1, and (iii) 3 h of irradiation (λ = 365 nm). The peaks correspond to the 16-nucleotide strands 5′-AGTTGACGGCATACGT-3′ in which a thymine dimer is present (elution time = 12.3 min) or absent (elution time = 15.5 min). The rhodium-modified oligonucleotide complement eluted at 29.9 min and is not shown here. The absolute yield of repaired strand varies somewhat from experiment to experiment, depending upon irradiation. (B) Long-range thymine dimer repair by a tethered rhodium intercalator in assembly **T<>T-2** over an 8-fold range of concentrations. Peaks in the HPLC chromatograms correspond to **T<>T-2** (elution time 10.2 min), repaired strand **2** (elution time 13.2 min) and the rhodium-tethered complementary strand (elution time = 29.4 min). Samples shown here, which are representative of the set, correspond to the following: (i) dark control; (ii) 25 μM rhodium and DNA duplex; (iii) 6.25 μM rhodium and DNA duplex. All samples except the dark control were irradiated for 1 h at 365 nm. The levels of repair are as follows: 25 μM: 82 ± 1%; 12.5 μM: 75 ± 1%; 6.25 μM: 70 ± 1%; 3.12 μM: 65 ± 5%, where the error bars represent the error in the integration due to noise. (C) Absence of dimer repair by a noncomplementary rhodium strand. A control solution containing a rhodium-modified strand (8 μM) and a noncomplementary strand (8 μM) containing a dimer was irradiated at 365 nm and only background repair is observed. Panel i shows the dark control sample which was not irradiated; the sample shown in panel ii was irradiated for 1 h; the sample shown in panel iii was irradiated for 3 h. The dimer strand (elution time = 11 min), the repaired strand (elution time = 13 min), and the rhodium-tethered strand (elution time = 26 min) are indicated by arrows. After 1 h, 2% of the dimer strands were repaired; after 3 h, 6% were repaired.

Table 1: Long-Range Guanine Damage in Duplexes with Tethered Rhodium

		G damage (%)[a]	
		1 h	3 h
TT-1	5′A-C-GG-CA-GTT-GA-T-A-CGT T-G-CCGT-CAA-CT-AT-Rh-GCA-5′	2	7
1	5′A-C-GG-CA-GT-T-GA-T-A-CGT T-G-CCGT-CA-A-CT-A-T-Rh-GCA-5′	4	10
TT-3	5′A-GTT-GA-C-GG-CA-T-A-CGT T-C-A-A-CT-GCCGT-AT-Rh-GCA-5′	1	4
3	5′A-GT-T-GA-C-GG-CA-T-A-CGT T-C-A-A-CT-GC-CGT-AT-Rh-GCA-5′	1.5	5

[a] Damage is expressed as the fraction of oligonucleotide (in percent) cleaved at guanine (site indicated by a vertical arrow) after 1 and 3 h of irradiation. Samples containing 8 μM duplex were irradiated at 365 nm and treated with aqueous piperidine prior to analysis by denaturing PAGE. Although the absolute accuracy of the measurements of guanine oxidation can vary by as much as 5% from experiment to experiment, the relative precision of these numbers is within 1%.

shows representative data and includes the full chromatogram with elution of the metalated strand. This range of concentrations was chosen to bracket the 8 μM duplex concentration used in these and previous dimer repair and guanine damage experiments. If the repair reaction were to proceed in a bimolecular fashion, assuming the interduplex repair efficiency to be comparable to that of nontethered Rh(phi)$_2$DMB^{3+}, it would require that the repair efficiency change by more than 500% over the concentration range examined. That the reaction occurs intraduplex is also evident in comparing the repair efficiency in the rhodium-tethered duplex to that for repair of the duplex containing the thymine dimer by a separate rhodium-modified duplex lacking the dimer. We observe ≤5% interduplex repair at a concentration of 8 μM.

DNA-mediated repair by charge transfer also requires that the intervening bases be paired. When a control solution containing a rhodium-modified strand (8 μM) and a noncomplementary strand (8 μM) containing a dimer was irradiated at 365 nm, essentially no repair is observed: after 1 h, 2% of the dimer strands were repaired; after 3 h, 6% were repaired (Figure 3C). The percent repair seen is comparable to the extent of dimer repair found upon irradiation without rhodium.

Dimer Repair by Rhodium in a Duplex Containing Guanine Doublets. Because initial oxidation of a 5′-GG-3′ site should be thermodynamically more favorable than oxidation of a thymine dimer, we considered the possibility that the guanine doublet would compete with the dimer for the migrating charge in duplexes containing both charge

Table 2: Long-Range Thymine Dimer Repair in Duplexes with Tethered Rhodium

		Thymine Dimer Repair (%)[a]		distance (Å)[b]	
		1 h	3 h	Rh-**T**-**T**	Rh-$^{5'}$G
TT-1	5′A-C-G-G-C-A-G-T-T-G-A-T-A-C-G-T T-G-C-C-G-T-C-A-A-C-T-A-T-Rh-G-C-A-5′	75	93	19	37
TT-2	5′A-G-C-G-C-A-G-T-T-G-A-T-A-C-G-T T-C-G-C-G-T-C-A-A-C-T-A-T-Rh-G-C-A-5′	94	100	19	
TT-3	5′A-G-T-T-G-A-C-G-G-C-A-T-A-C-G-T T-C-A-A-C-T-G-C-C-G-T-A-T-Rh-G-C-A-5′	53	70	36	20
TT-4	5′A-G-T-T-G-A-C-G-C-G-A-T-A-C-G-T T-C-A-A-C-T-G-C-G-C-T-A-T-Rh-G-C-A-5′	90	100	36	

[a] Repair is expressed as the percentage of thymine dimer lesion repaired after 1 and 3 h of irradiation. Samples containing 8 μM duplex were irradiated at 365 nm prior to analysis by HPLC. Repair efficiency is given for assemblies containing Δ-Rh. Although the absolute accuracy of the measurements of thymine dimer repair can vary considerably from experiment to experiment due to combined error in sample preparation, irradiation, and HPLC analysis, the relative precision of these numbers is approximately 5−10%. [b] Distances between Rh and the cyclobutane ring of the dimer and Rh and the 5′-G of the 5′-GG-3′ are based upon a 3.4 Å base-pair−base-pair separation and the intercalation positions shown schematically.

traps. Table 2 compares the dimer repair efficiency in four sequences with and without a guanine doublet. As expected, the presence of a 5′-GG-3′ site within the duplex diminished the efficiency of thymine dimer repair, as evidenced by the smaller yields for **T<>T-1** compared to **T<>T-2** and for **T<>T-3** compared to **T<>T-4**. The same diminution in efficiency in the presence of a 5′-GG-3′ doublet is evident in DNA assemblies containing tethered Λ rhodium, although the absolute yields of dimer repair were somewhat less for the Λ isomer (data not shown). Placement of the thymine dimer distal (36 Å) from intercalated rhodium in **T<>T-3** and **T<>T-4**, as opposed to proximal (19 Å), also reduced the repair efficiency.

Repair of a Thymine Dimer by a Ru(III) Intercalator. We showed that Ru(III) is generated in situ by irradiating Ru(phen)$_2$(dppz)$^{2+}$ in the presence of groove-bound oxidative quenchers, and that Ru(III), once generated, can oxidatively damage 5′-GG-3′ doublets (*40*, *41*). To determine whether Ru(III) could oxidatively repair a thymine dimer lesion, we prepared solutions containing a duplex with an identical sequence to **T<>T-1** (without tethered Rh), which contains both a centrally located thymine dimer and 5′-GG-3′ site, and a duplex with an identical sequence to **T<>T-2** (without tethered Rh), in which the guanine doublet had been removed. The assemblies were irradiated in the presence of Ru(phen)$_2$(dppz)$^{2+}$ and the oxidative quencher methyl viologen. Although on this time scale we observe significant thymine dimer repair by Rh(phi)$_2$DMB^{3+}, there was no evidence of thymine dimer repair by Ru(phen)$_2$(dppz)$^{2+}$ (Figure 4). Several new signals appear in the chromatograms concomitant with a small decrease in the amount of the strand containing the dimer. It is likely that these new signals correspond to oligonucleotide products containing oxidized guanine bases; guanines are known to be oxidized on this time scale, and the more heavily degraded strand corresponds to the strand containing the more easily oxidized sites (*40*). The same results were obtained with the electron-transfer quenchers Ru(NH$_3$)$_6^{3+}$ and Co(NH$_3$)$_3$Cl^{2+} (data not shown). In the absence of quencher, the strands are not oxidized, and only a small amount of background repair occurs.

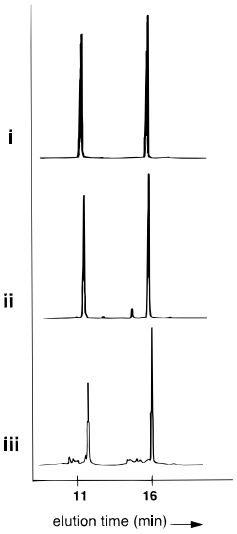

FIGURE 4: Absence of thymine dimer repair using a ruthenium intercalator and sequence **T<>T-1** (without tethered rhodium). Shown are the HPLC chromatograms: (i) dark control containing dimer-containing strand (elution time = 16 min) and the complementary strand (elution time = 11 min); (ii) irradiation at 436 nm without quencher for 45 min; (ii) irradiation at 436 nm with 10 equivalents of methyl viologen for 2 min.

Oxidation of Guanine by Ru(III) through an Intervening Thymine Dimer. Since Ru(III) cannot promote the repair a thymine dimer, we can use ruthenium intercalators to probe whether the dimer generates a disruption in the π-stack of the DNA duplex and how that disruption affects other electron-transfer reactions. We prepared an oligonucleotide

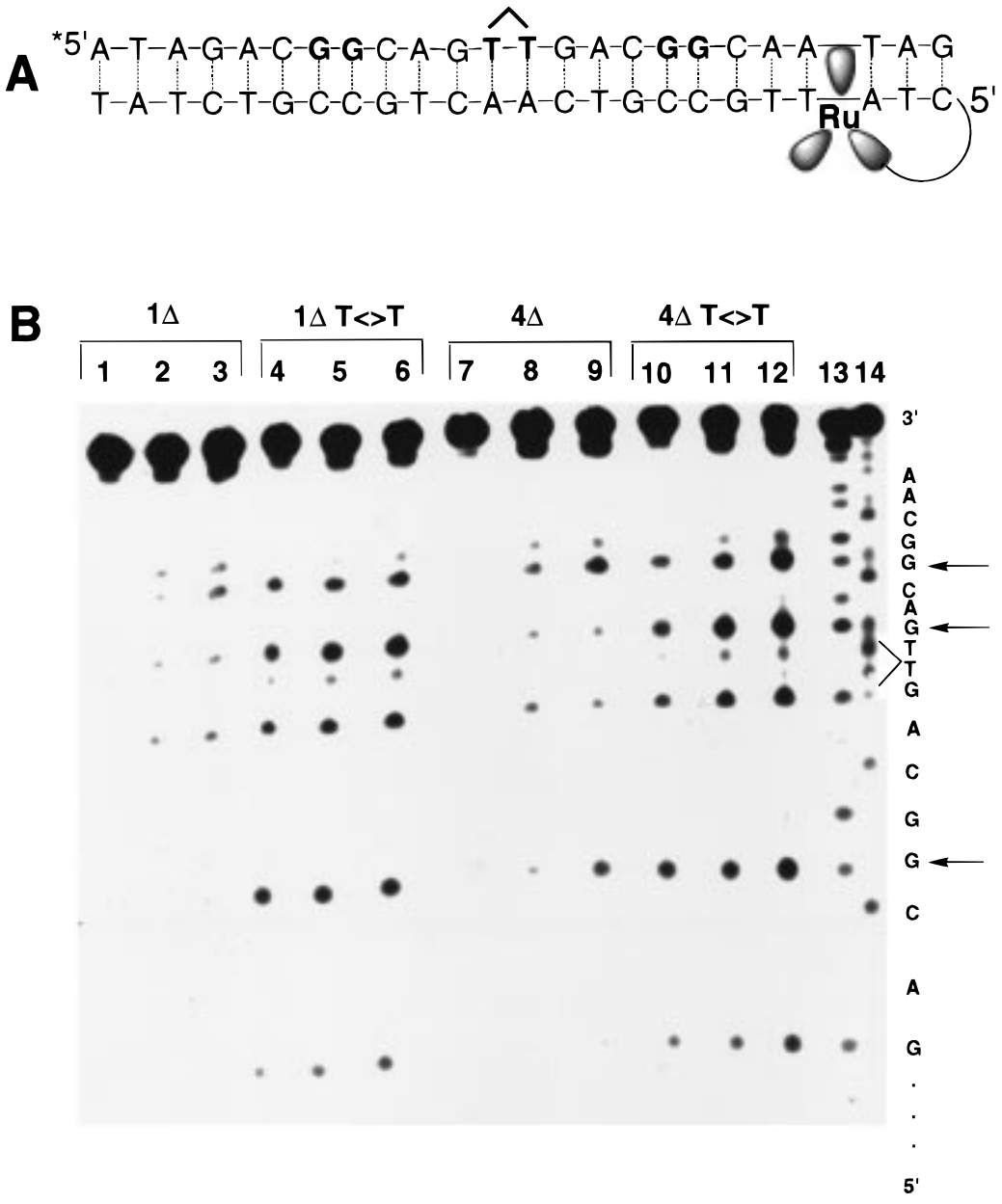

FIGURE 5: (A) Sequence **T<>T-5** with the location of the tethered ruthenium complex and the radioactive label indicated. (B) Autoradiogram of sequence **5** irradiated with 10 equivalents of methyl viologen^{2+} at 436 nm. The designations 1Δ and 4Δ correspond to the absolute configuration around the metal center and the order of elution of the metalated strand by HPLC. Samples were lanes 1−3, ruthenium isomer 1Δ irradiated for 0, 30, and 60 s without a dimer; lanes 4−6, isomer 1Δ irradiated for 0, 30, and 60 s with a thymine dimer; lanes 7−9, isomer 4Δ irradiated for 0, 30, and 60 s without a dimer; lanes 10−12, isomer 4Δ irradiated for 0, 30, and 60 s with a thymine dimer; lanes 13 and 14, Maxam−Gilbert sequencing lanes for A+G and C+T, respectively. Horizontal arrows denote the 5′-G of 5′-GG-3′ and the 3′-G of 5′-GTTG-3′ sites. Position of the thymine dimer lesion is denoted by brackets. Note that the levels of piperidine-sensitive damage are higher in all of the lanes containing the dimer including the dark control lanes; this background damage, which appears to originate from the synthesis of the thymine dimer by irradiation with triplet sensitizer, is subtracted out in the quantitation.

duplex containing tethered Ru(phen)(bpy′)(dppz)$^{2+}$, a centrally located thymine dimer site, and two 5′-GG-3′ sites located either proximally (17 Å) or distally (51 Å) from the tethered photooxidant. (Figure 5A) This sequence is analogous to that used to examine the effects of a DNA bulge upon electron transfer, in which a disruption is placed in the middle of a duplex with a guanine doublet on either side and a metallointercalator tethered to one end (*37*). By quantitating the ratio of the damage at the two guanine doublets in the absence versus the presence of an intervening thymine dimer, we can evaluate the influence of the disruption upon electron transfer through the helix.

Assemblies containing tethered ruthenium intercalators were irradiated at 436 nm, treated with aqueous piperidine, and analyzed by denaturing PAGE. The 5′-G of both guanine doublets as well as the 3′-G of the 5′-GT<>TG-3′ is damaged in all of the strands, as indicated by arrows. (Figure 5B) As in irradiations with Rh-tethered sequences **T<>T-1** and **T<>T-3**, quantitation revealed increased damage at the 3′-G of the 5′-GT<>TG-3′ in the presence of the dimer along with a concomitant decrease in the levels of damage at the 5′-Gs of the guanine doublets. Results for both of the Δ isomers of Ru(phen)(bpy′)(dppz)$^{2+}$ are the same.

DISCUSSION

Oxidative Repair of Thymine Dimers. The data presented here indicate clearly that visible photolysis of rhodium intercalators bound to DNA can promote the repair of a thymine dimer lesion. Product analysis indicates that the reaction proceeds to completion without significant side products being formed. The overall quantum yield for the reaction is low, which is understandable based upon the generally low efficiency of the rhodium photochemistry (*38*).

The Ru(III) species, generated in situ by oxidative quenching, promotes oxidative damage to DNA in a high-yield reaction without repairing the thymine dimer lesion. With an estimated reduction potential of $E_{1/2}([Ru]^{3+/2+}) \approx +1.6$V (*26*), Ru(III) is not sufficiently oxidizing to react with the thymine dimer. This conclusion is fully in line with estimates for oxidation of thymine dimer dinucleotides (*44*, *58*−*59*). Since the ruthenium complex can promote oxidative damage to DNA from a distance but cannot promote the repair of thymine dimer, it can be used to probe perturbations in DNA structure associated with the thymine dimer lesion (vide infra) (*36*, *37*).

An important issue with long-range thymine dimer repair by rhodium intercalators is whether the reaction is indeed mediated by the base pairs of the DNA double helix. One could imagine that the reaction proceeds instead in an interduplex fashion, with the rhodium complex from one duplex intercalating into a neighboring duplex at the site of the thymine dimer and initiating its repair. This is especially important to consider because repair by a noncovalent bound rhodium intercalator is more than an order of magnitude more efficient than repair by rhodium tethered to the end of the duplex (*55*). Several experiments rule out an interduplex reaction. Photocleavage reactions with 313 nm light indicate that interduplex intercalation is negligible at duplex concentrations of $\leq 25\ \mu$M. If the rhodium complexes intercalate into neighboring duplexes and repair the dimer in an intermolecular reaction, the photocleavage reactions at 313 nm would show damage throughout the DNA strands. The photocleavage reactions instead indicate that intercalation occurs predominantly at the end of the duplex nearest to the tethered rhodium. Direct photocleavage studies of DNA duplexes containing a thymine dimer by noncovalently bound $Rh(phi)_2DMB^{3+}$ also provide no indication of preferential intercalation neighboring the thymine dimer. Furthermore, if the repair reaction occurs in an interduplex fashion, the yield of repaired dimer would increase substantially as the concentration of the rhodium-tethered duplex was increased. Instead, the level of repair observed as a function of concentration is consistent with an interduplex dimerization constant of $\leq 10^3\ M^{-1}$. Last, that the reaction occurs intraduplex is illustrated simply by the observation that little repair is detected in solutions containing duplexes with thymine dimers but no rhodium mixed with duplexes lacking a thymine dimer but with tethered rhodium. The rhodium intercalator must be bound to a DNA duplex containing the thymine dimer for the reaction to proceed.

A question that remains is why the efficiency of repair by noncovalently bound rhodium exceeds that of the tethered rhodium by more than an order of magnitude. Increasing the separation between the thymine dimer and the rhodium intercalator actually increases the efficiency of repair (*55*), so the different separations of the intercalated and nonintercalated rhodium from the thymine dimer cannot account for this effect. It seems unlikely that the redox potential for the tethered rhodium complex differs sufficiently from that for rhodium noncovalently bound to account for this discrepancy. One might consider that the noncovalently bound intercalator binds preferentially in the vicinity of the thymine dimer. Photocleavage data provide no evidence for such preferential binding, however. Another possibility is that the thymine dimer, tethered rhodium intercalator, or both are not optimally oriented within the DNA duplex compared to that for the rhodium noncovalently bound to the helix. In this context, it is noteworthy that although the efficiency of thymine dimer repair differs so much using tethered and noncovalently bound rhodium, the efficiency of guanine oxidation is comparable for tethered versus nontethered rhodium (*38*).

Disturbances in Duplex DNA Generated by the Thymine Dimer. What perturbations in DNA structure are associated with the thymine dimer, and can structural distortions be detected in these oxidative reactions? We observed that the location of the dimer within the short pieces of duplex DNA affected the yield of dimer repair (Table 2). Placement of the thymine dimer distal (36 Å) from intercalated rhodium, as opposed to proximal (19 Å), reduces the repair efficiency. Although this might reflect the increased distance between the reactants, it is also possible that the effect of position in the duplex may be caused by thermodynamic destabilization and destacking near the dimer when it resides at the end of the assembly (**T<>T-3**, **T<>T-4**) rather than at its center (**T<>T-1**, **T<>T-2**). In smaller duplexes with the thymine dimer in the center of the helix, repair efficiency increases with increasing duplex length (*55*). We have observed that the efficiency of electron transfer is related to the stacking of the base pairs in the DNA duplex: disruptions in the DNA caused by bulges reduce thymine dimer repair efficiency and guanine oxidation on the far side of the disruption, presumably by disturbing electron transfer through that part of the duplex (*37*, *55*). Fraying at the ends of the duplex may disrupt stacking in a similar way, causing the diminution in repair efficiency for dimers located near the ends of the duplex.

Furthermore, the thymine dimer changes the chemical reactivity of bases in its vicinity. We noted that the 3′-G of the sequence 5′-GT<>TG-3′ is preferentially oxidized by rhodium in the presence of the thymine dimer, with a concomitant decrease in the damage at the 5′-G of 5′-GG-3′ sites. The same phenomenon is observed with the ruthenium oxidant which cannot repair the dimer. The ratio of the damage at a distal guanine doublet versus a proximal doublet remains constant, however, indicating that putative structural perturbations introduced by the dimer do not block the migration of a charge *through* the helix. Since the structure of the thymine dimer within a duplex is still under debate (*76*−*79*), it is unclear whether the charge is transported through the strand opposite the dimer or through the dimer itself, given that the dimer would have to be stacked into the helix in order to be electronically coupled to the other bases. However, the thymine dimer is not aromatic, and it is unlikely that a nonaromatic ring would be well-coupled even if it were well stacked. This increased sensitivity of the 3′-G to oxidation, relative to controls having identical

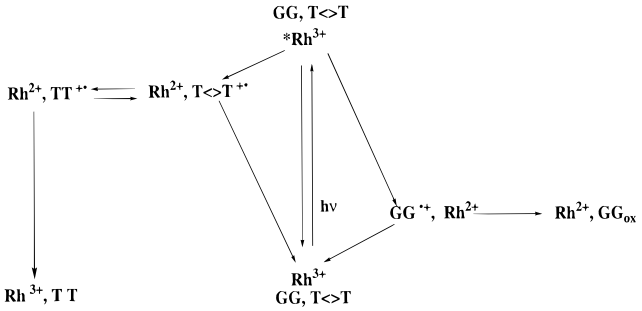

FIGURE 6: Proposed mechanisms for thymine dimer repair and guanine oxidation by an excited-state rhodium oxidant. When excited by light, the rhodium complex can oxidize guanine doublets or thymine dimers or return to the ground state. The oxidized thymine dimer radical cation intermediate can then undergo cycloreversion to a radical cationic form of the native thymines, which then oxidize the Rh^{2+}. The back reaction can also occur: the dimer radical cation intermediate can also oxidize the Rh^{2+} directly and return to the ground state. Alternatively, the 5′-G of the guanine doublet can be oxidized by $*Rh^{3+}$. The oxidized guanine radical cation can then undergo a trapping reaction with water or oxygen to form 8-oxo-dG (G_{ox}), or the back reaction can occur. Transfer of the electronic hole between the dimer radical cation and the guanine and/or between the guanine cation radical and the dimer may also be possible, although the energetics make the latter unlikely (not shown).

base sequence but no thymine dimer (lanes 4, 5 and 12, 13), is reminiscent of increased sensitivity to long-range damage which we observed previously at single base mismatch sites (*40*). These data indicate that structural changes caused by the dimer either (i) increase the accessibility of the 3′-G of the 5′-GT<>TG-3′ tetrad to molecular oxygen, (ii) alter its redox potential, (iii) increase the residence time of the excited electron hole at the site, or (iv) generate some combination of these factors. Certainly the observation of preferential oxidation to one side of the dimer reflects that some local structural distortion has occurred and that the distortion is asymmetric.

Factors Governing Simultaneous Dimer Repair and Guanine Oxidation. Because photolysis of the rhodium complex can promote both oxidative damage to DNA and the repair of a thymine dimer, we can examine how these two sites for oxidative reaction on DNA compete electronically within the DNA helix. Figure 6 summarizes the various competing reactions which are involved.

Photoexcitation of $Rh(phi)_2DMB^{3+}$ at 400 nm gives rise to an intraligand charge-transfer state on the phi with a reduction potential of $E_{1/2}([Rh]^{3+*/2+}) \approx +2.0$ V versus NHE (*80*), which is of sufficient potential to oxidize the thymine dimer. In contrast, ground-state Ru(III), with a less positive estimated reduction potential [$E_{1/2}([Ru]^{3+/2+}) \approx +1.6$ V versus NHE] (*26*), cannot oxidize the thymine dimer. This brackets the oxidation potential of the thymine dimer within a DNA duplex as +1.6−2.0 V. Thymine dimer repair by rhodium involves oxidation and collapse of the cyclobutane ring. Since we have demonstrated that catalytic amounts of rhodium, noncovalently bound, can be used to repair thymine dimers (*55*), we know that the oxidative repair of the dimer by rhodium is simply triggered by electron transfer. Also, the lifetime of the dimer cation must be on the order (or shorter lived) than the reduced rhodium, which is known to undergo decomposition on the microsecond time scale. Chemically induced dynamic nuclear polarization (CIDNP) studies on thymine dimer model compounds reveal that the dimer cation radical intermediate has a lifetime of <200 ns, although the rate of the initial charge trapping event has not been bracketed (*81*). The presence of the surrounding DNA duplex may affect that lifetime, however.

Both *Rh(III) and Ru(III) intercalators oxidize guanine selectively at the 5′-G of 5′-GG-3′ sites. Although the electrochemical properties of guanine in duplex DNA are not explicitly known, the oxidation potential of guanine was estimated by pulse radiolysis in neutral aqueous solution to be +1.29 V (*56*), which is less than the reduction potential of both ruthenium(III) and photoexcited rhodium(III). The quantum yield for oxidation by the "flash-quench" method with ruthenium complexes is higher than that for the direct photooxidation by the rhodium excited state, leading to a much higher yield of oxidized guanine in the same sequence over the same irradiation times. Although guanine oxidation is thermodynamically more favorable than thymine dimer repair, the former reaction involves multiple bimolecular reactions that trap the damage irreversibly. In fact, the quantum yield of guanine oxidation is substantially lower than for dimer repair by tethered rhodium (5×10^{-8} versus at 365 versus 2×10^{-6} at 400 nm, respectively). Damage to guanine by metallointercalators is thought to proceed via initial oxidation of the base in ≤200 ns, giving the guanine cation radical which is quickly deprotonated to form the neutral guanine radical [G•(−H)]. The neutral guanine radical subsequently reacts with an oxygen source, likely O_2, on the microsecond time or longer scale to form stable oxidation products (*41*). With both rhodium and ruthenium intercalators, the thermodynamics of the initial oxidation, lifetime of the guanine radical intermediate(s), rate of back electron transfer, and rate of oxygen trapping to provide damaged products can all potentially contribute to the damage yields.

In duplexes containing only thymine dimers, dimer repair occurs with high yield regardless of its location with respect to the metallointercalator. When the thymine dimer lesion and a guanine doublet are both present in an assembly containing tethered rhodium, the level of repair decreases. Clearly, guanine oxidation is thermodynamically favored over dimer repair. The fact that dimer repair and guanine oxidation can compete for the mobile charge indicates that the charge is equilibrated across the entire duplex. The fact that the relative position of the guanine doublet and the dimer lesion with respect to the oxidant does not affect the product outcome provides further evidence for this assertion. We have seen equilibration across the duplex before, by the formation of oxidized product by Ru(III) at all sites of equivalent oxidation potential in the absence of a guanine doublet "sink" (*40*).

In duplexes containing only guanine traps, oxidative damage and charge trapping occur at the most easily oxidized sites, independent of location with respect to the tethered oxidant (*36*). When both a thymine dimer and guanine doublet are present in an assembly containing tethered rhodium, the amount of oxidized guanine formed decreases. Although a dimunition in the levels of guanine oxidation could in principle be caused by a destabilization in the helix induced by the dimer, we can eliminate this possibility because the amount of guanine oxidized by Ru(III) is not diminished by the presence of the thymine dimer. Therefore,

the thymine dimer must instead be depleting the system of the electronic holes which lead to the formation of oxidized guanine. Guanine oxidation is thermodynamically favored over thymine dimer repair by ~400 mV, which corresponds to an equilibrium constant for the equilibrium between oxidized guanine and oxidized dimer of 5×10^6. The collapse of the dimer cation radical to two repaired thymines must occur faster than the trapping of the guanine cation radical by an oxygen source. What controls the formation of the two products is not then simply the thermodynamic difference between the guanine and the dimer but also the difference in lifetimes and reactivity between the guanine radical (microseconds to milliseconds) and dimer cation radical intermediate (~200 ns). Furthermore, given that the order within the sequence does not affect the identity of the products, we may conclude that the equilibration must be faster than the trapping reactions of either the guanine radical or the dimer radical.

Our results therefore point to rapid equilibration of the oxidizing charge throughout the duplex on a time scale which is fast relative to the charge-trapping event. Both hopping mechanisms and delocalized band models have been used to describe the movement of charges through DNA. In a hopping mechanism, an electron or electronic hole is localized on a particular base and migrates from base to base in discrete "hops", each hop independent of the previous one (*1*). The hopping rate is significantly faster than vibrational relaxation, allowing the charge to diffuse away from the site at which it is generated before it is trapped. When a hopping mechanism is used to explain the movement of the oxidizing charge across the duplex, one difficulty arises: how can an electronic hole hop *up* (energetically) to a thymine dimer from the neighboring bases, which have much lower oxidation potentials? We must invoke an excited electron or electronic hole with sufficient energy to oxidize all of the bases before relaxation in order for a hopping mechanism to describe our results, which clearly show the oxidation of both thymine dimers and guanine doublets located distal to the dimers. Alternatively, a delocalized band model may be considered to describe the equilibration of an oxidizing charge throughout the duplex. In this model, the DNA is described like other conducting polymers, with bands of many overlapping electronic states in the place of individual HOMOs and LUMOs into which electrons can be injected or from which electrons can be withdrawn. Perhaps some combination of hopping and delocalized band formation is needed in the development of models which accurately describe the migration of charges through DNA.

Implications with Respect to Biological Charge Transport Mediated by DNA. Viewed classically, chemical modification of a particular DNA sequence in the genome requires direct contact between a sequence and the agent which carries out the chemistry. Here we demonstrate, however, that sequence-selective chemical transformations of DNA can be induced remotely by charge transfer without direct physical contact between the oxidant and the reactive base(s) on the DNA. The reacting partner, the tethered metallointercalator, binds to DNA at a position spatially separated from the reactive 5′-GG-3′ and thymine dimer sites, initiating chemistry at a distance. Moreover, the efficiency of one reaction is affected by the presence of the other. Different sites on the DNA duplex can compete electronically.

Although we now possess evidence for both long-range DNA damage and repair in vitro, we have no indication that analogous reactions occur in the cell. Certainly, the possible application of rhodium photochemistry for the therapeutic repair of thymine dimer lesions would have to take into account the irreversible damage to guanine sites which also occurs. Perhaps, however, the chemotherapeutic utility of this chemistry lies instead in suggesting a different strategy for the design of DNA-targeted therapeutics, one based upon performing chemistry from a distance. This notion may also provide a new perspective in understanding some mechanisms of action of redox active natural product chemotherapeutic agents which are utilized currently.

ACKNOWLEDGMENT

We are grateful to D. Hall, R. E. Holmlin, and E. Stemp for helpful discussions.

REFERENCES

1. Dee, D., and Baur, M. E. (1974) *J. Chem. Phys. 60*, 541−560.
2. Bernhard, W. A. (1989) *J. Phys. Chem. 93*, 2187−2189.
3. Bernhard, W. A., Barnes, J., Mercer, K. R., and Mroczka, N. (1994) *Radiat. Res. 140*, 199−214.
4. Cullis, P. M., McClymont, J. D., and Malone, M. E. (1992) *J. Chem. Soc., Perkin. Trans. 10*, 1695−1702.
5. Gregoli, S., Olast, M., and Bertinchamps, A. (1979) *Radiat. Res. 70*, 417−431.
6. Hüttermann, J., Voit, K., Oloff, H., Köhnlein, W., Gräslund, A., and Rupprecht, A. (1984) *Faraday Discuss. Chem. Soc. 78*.
7. Melvin, T., Plumb, M. A., Botchway, S. W., P. O'Neill, P., and Parker, A. W. (1995) *Photochem. Photobiol. 61*, 584−591.
8. Melvin, T., Botchway, S. W., Parker, A. W., and O'Neill, P. (1996) *J. Am. Chem. Soc. 118*, 10031−10036.
9. Sevilla, M. D., Becker, D., Yan, M., and Summerfield, S. R. (1991) *J. Phys. Chem. 95*, 3409−3415.
10. Al-Kazwini, A. T., O'Neill, P., Adams, G. E., and Fielden, E. M. (1990) *Radiat. Res. 121*, 149−153.
11. Anderson, R. F., Patel, K. B., and Wilson, W. R. (1991) *J. Chem. Soc., Faraday Trans. 1 87*, 3739−3746.
12. Cullis, P. M., McClymont, J. D., and Symons, M. C. R. (1990) *J. Chem. Soc., Faraday Trans. 86*, 591−592.
13. Pezeshk, A., Symons, M. C. R., and McClymont, J. D. (1996) *J. Phys. Chem. 100*, 18562−18566.
14. O'Neill, P., and Fielden, E. M. (1993) *Adv. Radiat. Biol. 17*, 53−120.
15. Atherton, S. J., and Beaumont, P. C. (1995) *J. Phys. Chem. 99*, 12025−12029.
16. Baguley, B. C., and LeBret, M. (1984) *Biochemistry 23*, 937−943.
17. Brun, A. M., and Harriman, A. (1991) *J. Am. Chem. Soc. 113*, 8153−8159.
18. Brun, A. M., and Harriman, A. (1992) *J. Am. Chem. Soc. 114*, 3656−3660.
19. Brun, A. M., and Harriman, A. (1994) *J. Am. Chem. Soc. 116*, 10383−10393.
20. Davis, L. M., Harvey, J. D., and Baguley, B. C. (1987) *Chem. Biol. Interact. 62*, 45−58.
21. Fromherz, P., and Rieger, B. (1986) *J. Am. Chem. Soc. 108*, 5361−5362.
22. Kelley, S. O., Holmlin, R. E., Stemp, E. D. A., and Barton, J. K. (1997) *J. Am. Chem. Soc. 119*, 9861−9870.
23. Lewis, F., Wu, T., Zhang, Y., Letsinger, R., Greenfield, S., and Wasielewski, M. (1997) *Science 277*, 673−676.
24. Manoharan, M., Tivel, K. L., Zhao, M., Nafisi, K., and Netzel, T. L. (1995) *J. Phys. Chem. 99*, 17461−17472.

25. Meade, T. J. (1996) in *Metal Ions in Biological Systems* (Sigel, A., and Sigel, H., Eds.) pp 453, Marcel Dekker, Inc., New York.
26. Murphy, C. J., Arkin, M. R., Ghatlia, N. D., Bossmann, S., Turro, N. J., and Barton, J. K. (1994) *Proc. Natl. Acad. Sci. U.S.A. 91*, 5315−5319.
27. Nordén, B., Lincoln, P., Akerman, B., and Tuite, E. (1996) in *Metal Ions in Biological Systems* (Sigel, A., and Sigel, H., Eds.) pp 177, Marcel Dekker, Inc., New York.
28. Stemp, E. D. A., and Barton, J. K. (1996) in *Metal Ions In Biological Systems* (Sigel, A., and Sigel, H., Eds.) pp 325−365.
29. Armitage, B., Yu, C., Devadoss, C., and Schuster, G. B. (1994) *J. Am. Chem. Soc. 116*, 9847−9859.
30. Breslin, D., Coury, J., Anderson, J., McFail-Isom, L., Kan, Y., Williams, L. D., Bottomley, L., and Schuster, G. B. (1997) *J. Am. Chem. Soc.* 5043−5044.
31. Breslin, D., and Schuster, G. B. (1996) *J. Am. Chem. Soc. 118*, 2311−2319.
32. Ly, D. K., Y., Armitage, B., and Schuster, G. B. (1996) *J. Am. Chem. Soc. 118*, 8747−8748.
33. Saito, I., Takayama, M., Sugiyama, H., Nakatani, K., Tsuchida, A., and M. Yamamoto. (1995) *J. Am. Chem. Soc. 117*, 6406−6407.
34. Dunn, D. A., Lin, V. H., and Kochevar, I. E. (1992) *Biochemistry 31*, 11620−11625.
35. Ito, K., Inoue, S., Yamamoto, K., and Kawanishi, S. (1993) *J. Biol. Chem. 268*, 13221−13227.
36. Hall, D. B. (1997) Ph.D. Thesis, California Institute of Technology.
37. Hall, D. B., and Barton, J. K. (1997) *J. Am. Chem. Soc. 119*, 5045.
38. Hall, D. B., Holmlin, R. E., and Barton, J. K. (1996) *Nature 382*, 731−735.
39. Sugiyama, H., and Saito, I. (1996) *J. Am. Chem. Soc. 118*, 7063−7068.
40. Arkin, M. R., Stemp, E. D. A., Pulver, S. C., and Barton, J. K. (1997) *Chem. Biol. 4*, 389−400.
41. Stemp, E. D. A., Arkin, M. R., and Barton, J. K. (1997) *J. Am. Chem. Soc. 119*, 2921.
42. Sancar, A. (1996) *Annu. Rev. Biochem. 65*, 43−81.
43. Begley, T. P. (1994) *Acc. Chem. Res. 27*, 394−401.
44. Heelis, P. F., Hartman, R. F., and Rose, S. D. (1995) *Chem. Soc. Rev. 24*, 289.
45. Kim, S.-T., and Sancar, A. (1993) *Photochem. Photobiol. 57*, 895−904.
46. Sancar, A. (1994) *Biochemistry 33*, 2−9.
47. Taylor, J. S. (1994) *Acc. Chem. Res. 27*, 76−82.
48. Charlier, M., and Hélène, C. (1975) *Photochem. Photobiol. 21*, 31−37.
49. Hélène, C., and Charlier, M. (1977) *Photochem. Photobiol. 25*, 429−434.
50. Jacobsen, J. R., Cochran, A. G., Stephans, J. C., King, D. S., and Schultz, P. G. (1995) *J. Am. Chem. Soc. 117*, 5453−5461.
51. Kim, S.-T., Hartman, R. F., and Rose, S. D. (1990) *Photochem. Photobiol. 52*, 789−794.
52. Kim, S.-T., and Rose, S. D. (1990) *J. Phys. Org. Chem. 3*, 581−586.
53. Carell, T., Epple, R., and Gramlich, V. (1996) *Angew. Chem., Int. Ed. Engl. 35*, 620−623.
54. Epple, R., Wallenborn, E.-U., and Carell, T. (1997) *J. Am. Chem. Soc. 119*, 7440−7451.
55. Dandliker, P. J., Holmlin, R. E., and Barton, J. K. (1997) *Science 275*, 1465−1468.
56. Steenken, S., and Jovanovic, S. V. (1997) *J. Am. Chem. Soc. 119*, 617−618.
57. Heelis, P. F., Deeble, D. J., Kim, S.-T., and Sancar, A. (1992) *Int. J. Radiat. Biol. 62*, 137−143.
58. Pac, C., Kubo, J., Tetsuro, M., and Sakurai, H. (1982) *Photochem. Photobiol. 36*, 273−282.
59. Wayner, D. D. M. (1989) in *Handbook of Organic Photochemistry* (Sca'iano, J. C., Ed.) pp 363−369, CRC Press, Boca Raton.
60. Beaucage, S. L., and Caruthers, M. H. (1981) *Tetrahedron Lett. 22*, 1859−1802.
61. Caruthers, M., Beaton, G., Wu, J. V., and Wiesler, W. (1992) *Methods Enzymol. 211*, 3−20.
62. Goodchild, J. (1990) *Bioconjugate Chem. 1*, 165−187.
63. Amouyal, E., Homsi, A., Chambron, J. C., and Sauvage, J. P. (1990) *J. Chem. Soc., Dalton Trans. 6*, 1841−1845.
64. Anderson, P. A., Deacon, G. B., Haarmenn, K. H., Keene, F. R., Meyer, T. J., Reitsma, D. A., Skelton, B. W., Strouse, G. F., Thomas, N. C., Treadway, J. A., and Whit, A. H. (1995) *Inorg. Chem. 34*, 6145−6157.
65. Friedman, A. E., Chambron, J.-C., Sauvage, J.-P., Turro, N. J., and Barton, J. K. (1990) *J. Am. Chem. Soc. 112*, 4960−4962.
66. Banerjee, S. K., Borden, A., Christensen, R. B., LeClerc, J. E., and Lawrence, C. W. (1990) *J. Bacteriol. 172*, 2105−2112.
67. Banerjee, S. K., Christensen, R. B., Lawrence, C. W., and LeClerc, J. E. (1988) *Proc. Natl. Acad. Sci. U.S.A. 85*, 8141−8145.
68. Setlow, J. K. (1966) in *Current Topics in Radiation Research* (Ebert, M., and Howard, A., Eds.) pp 197−248, North-Holland, Amsterdam.
69. Lippke, J. A., Gordon, L. K., Brash, D. E., and Haseltine, W. A. (1981) *Proc. Natl. Acad. Sci. U.S.A. 78*, 3388−3392.
70. Wachter, L., Jablonski, J.-A., and Ramachandran, K. L. (1986) *Nucleic Acids Res. 14*, 7985−7994.
71. Dupureur, C. M., and Barton, J. K. (1997) *Inorg. Chem. 36*, 33−43.
72. Sambrook, J., Fritsch, E. F., and Maniatis, T. (1989) *Molecular Cloning: A Laboratory Manual*, 2nd ed., Cold Spring Harbor Laboratory, New York.
73. Pyle, A. M., Long, E. C., and Barton, J. K. (1989) *J. Am. Chem. Soc. 111*, 4520−4522.
74. Sitlani, A., and Barton, J. K. (1994) *Biochemistry*, 12100−12108.
75. Sitlani, A., Long, E. C., Pyle, A. M., and Barton, J. K. (1992) *J. Am. Chem. Soc. 114*, 2303−2312.
76. Cooney, M. G., and Miller, J. H. (1997) *Nucleic Acids Res. 25*, 1432−1436.
77. Kemmink, J., Boelens, R., Koning, T., Vandermarel, G. A., Vanboom, J. H., and Kaptein, R. (1987) *Nucleic Acids Res. 15*, 4645−4653.
78. Taylor, J. S., Garrett, D. S., Brockie, I. R., Svoboda, D. L., and Telser, J. (1990) *Biochemistry 29*, 8858−8866.
79. Miaskiewicz, K., Miller, J., and Cooney, M. (1997) *J. Am. Chem. Soc. 119*, 9156−9163.
80. Turro, C., Enenzahav, A., Bossmann, S. H., Barton, J. K., and Turro, N. J. (1996) *Inorg. Chim. Acta 243*, 101−108.
81. Kemmink, J., Eker, A. P. M., and Kaptein, R. (1986) *Photochem. Photobiol. 44*, 137−142.

BI980041W